

NUMERICAL STUDY OF VISCOUS EFFECTS ON ACOUSTIC WAVES

N. MOHD. GHAZALI*

Abstract. A two-dimensional numerical simulation of acoustic waves in a closed rectangular acoustic chamber is completed. Numerical computations are performed by solving the two-dimensional, unsteady, viscous, non-linear Navier-Stokes system of equations. Finite difference methodology was used accurate to second order both in time and space. No-slip, no through flow and zero heat flux are set boundary conditions. Acoustic waves are generated by a vibrating membrane or piston on one wall. Computations are completed for variation in viscosity of the fluid. Results of the temperature profiles seem to agree with analytical solutions for a standing wave in an enclosure and those obtained experimentally with low perturbation to mean pressure ratio. Temperature nodes and anti-nodes each was found to occur near walls and midway through the chamber respectively, results associated with a half wavelength standing wave.

Key words: numerical study, acoustic waves, membrane, piston

Abstrak. Simulasi kaedah berangka 2-dimensi telah dilakukan terhadap gelombang akustik di dalam kebuk akustik tertutup segi empat tepat. Penyelesaian dilakukan terhadap persamaan sistem tak lurus Navier-Stokes 2-dimensi, aliran tak mantap dengan kelikatan yang berbeza. Kaedah perbezaan tak terhingga digunakan dengan kejituan tertib dua terhadap masa dan ruang. Sempadan halaju ialah tanpa gelincir dan tanpa telus aliran, dengan fluks haba sifar pada dinding kebuk. Gelombang akustik dihasilkan oleh pemacu akustik selaput atau omboh yang terletak pada salah satu dinding menegak. Suhu hasil kajian didapati sama dengan penyelesaian teori dan ujikaji untuk gelombang akustik di dalam suatu kebuk tertutup. Nod suhu (minimum) dan antinod suhu (maksimum) masing-masing wujud pada dinding dan di tengah kebuk.

Kata kunci: Kajian berangka, gelombang akustik, selaput, omboh

1.0 INTRODUCTION

Recent interest has been generated towards the study of interactions of acoustic waves with solid boundaries, thermoacoustic phenomena, due to the newly discovered use of the effects. Oscillations induced by a temperature gradient and temperature gradients induced by oscillations promise a new heat engine technology. The former can be used to run the latter without any hazardous environmental impact.

Thermoacoustics was first observed by European glass blowers over two hundred years ago. Sound is sometimes heard as a heat source is placed on one end of a cold

* Faculty of Mechanical Engineering, Universiti Teknologi Malaysia, 81310 UTM Skudai, Johor, Malaysia.
Email : normah@fkm.utm.my

glass tube. The theory was discussed qualitatively by Lord Rayleigh in 1877 [1]. Quantitative analysis, however, was done in 1980 by Rott [2]. A thermoacoustic heat engine basically runs like the heat engine that are taught in the introductory thermodynamics courses. Heat flows from a high temperature reservoir to a low temperature reservoir, generating acoustic power in a thermoacoustic prime mover. A thermoacoustic refrigeration or heat pump requires acoustic work to transfer heat from a low temperature heat source to a high temperature heat sink. The first and second law of thermodynamics still applies to the heat engines, with the highest performance being the Carnot performance.

The thermoacoustic effect can be best explained in a Lagrangian point of view, seen here in Figure 1. As the fluid element (A) on the left that is next to a solid boundary in an initially isothermal enclosure is compressed, its temperature rises. Having a temperature higher than the solid, heat is transferred from the element (B) to the solid. During expansion, the particle returns to its initial position. It now has a lower temperature than the solid and heat is accepted from the solid next to it. Over time and a finite length of solid, a temperature gradient is developed across the plate. The limit to this temperature gradient is the thermal conductivity of both the fluid and the solid.

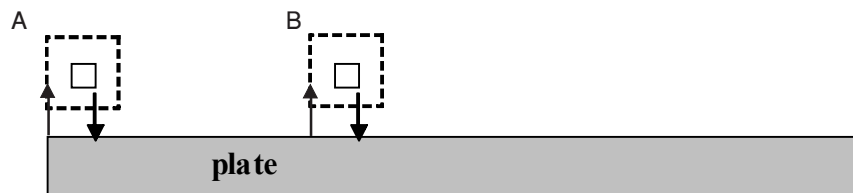


Figure 1 Lagrangian view of thermoacoustic effects

Since thermoacoustic theory is relatively new, studies are being done to better understand the concept and explain the factors that may or may not influence the solid-fluid interactions in an acoustic chamber. Analytical solution to the non-linear viscous compressible flow that described the acoustic waves in an enclosure is limited to the simple one-dimensional problem. This report is part of a numerical study of acoustic waves in a rectangular chamber. The waves are generated by a piston or membrane, typical acoustic drivers used in practical thermoacoustic chambers.

2.0 GOVERNING EQUATIONS

The governing equations are the Navier-Stokes system assuming Newtonian fluid with constant thermophysical properties.

$$\frac{D\rho}{Dt} = \rho (\nabla \cdot \mathbf{u}) = 0 \quad (1)$$

$$\rho \left(\frac{\partial u}{\partial t} + (u \cdot \nabla) u \right) = -\nabla p + \mu \nabla^2 u + \frac{\mu}{3} \nabla (\nabla \cdot u), \quad (2)$$

$$\rho c_p \frac{DT}{Dt} = \nabla \cdot (K \nabla T) + \frac{Dp}{Dt} + \mu \Phi, \quad (3)$$

where Φ term [3] has been dropped in this study. Ideal gas behavior is assumed. The above equations are nondimensionalized using the height of the acoustic chamber, H , and the circular frequency of forcing, ω . Manipulations of the equations are done to remove pressure from the linear terms. The resulting system of equations is [4]

$$\begin{aligned} \frac{\partial^2 u}{\partial t^2} &= \frac{1}{M^2 \gamma} \left(\frac{\partial^2 u}{\partial x^2} + \frac{\partial^2 v}{\partial x \partial y} - \frac{\partial^2 T}{\partial x \partial t} \right) + \frac{1}{\text{Re}} \frac{\partial}{\partial t} (\nabla^2 u) \\ &+ \frac{1}{3\text{Re}} \frac{\partial}{\partial t} \left(\frac{\partial^2 u}{\partial x^2} + \frac{\partial^2 v}{\partial x \partial y} \right) + \frac{1}{M^2 \gamma} \frac{\partial}{\partial x} (Q_p) - \frac{\partial}{\partial t} (Q_x), \end{aligned} \quad (4)$$

$$\begin{aligned} \frac{\partial^2 v}{\partial t^2} &= \frac{1}{M^2 \gamma} \left(\frac{\partial^2 u}{\partial x \partial y} + \frac{\partial^2 v}{\partial y^2} - \frac{\partial^2 T}{\partial y \partial t} \right) + \frac{1}{\text{Re}} \frac{\partial}{\partial t} (\nabla^2 v) \\ &+ \frac{1}{3\text{Re}} \frac{\partial}{\partial t} \left(\frac{\partial^2 u}{\partial x \partial y} + \frac{\partial^2 v}{\partial y^2} \right) + \frac{1}{M^2 \gamma} \frac{\partial}{\partial y} (Q_p) - \frac{\partial}{\partial t} (Q_y), \end{aligned} \quad (5)$$

$$\frac{\partial T}{\partial t} = \frac{\gamma}{Pe} \nabla^2 T + (1 - \gamma) (\nabla \cdot u) + (1 - \gamma) Q_p - \gamma Q_T, \quad (6)$$

$$\frac{\partial p}{\partial t} = \frac{\gamma}{\gamma - 1} \left(\frac{\partial T}{\partial t} - \frac{1}{Pe} \nabla^2 T + Q_T \right), \quad (7)$$

where the subscripted Q_s contain the non-linear terms. Three dimensionless expressions, the Reynolds number, Mach number, and Peclet number, have been introduced into the dimensionless system of equations. They are defined as

$$\text{Re} = \frac{H^2 \omega}{\nu}, \quad (8)$$

$$M = \frac{H \omega}{\sqrt{\gamma R T_m}}, \quad (9)$$

$$Pe = \frac{H}{\alpha} \omega, \quad (10)$$

with ν being the viscosity, γ the isobaric specific heat, R the gas constant, α the thermal diffusivity, and T_m the average temperature in the resonator.

3.0 NUMERICAL FORMULATIONS

The system of Equations (4)–(7) is then turned into algebraic equations using finite difference methodology. Spatial interior grid points used central differences, and one-sided derivatives are used on the boundaries [5]. The temporal integration is achieved with a semi-implicit method where the linear terms are treated implicitly, and the nonlinear terms explicitly. The linear terms in the equations containing first order temporal derivatives are treated with the Crank-Nicholson method in the usual manner. The nonlinear terms are treated with the Adams-Bashforth method. The equations are accurate to second order both spatially and temporally. Boundary conditions are zero heat flux with no-flow through and no-slip for the axial and vertical velocities normal to the walls,

$$v(0, y, t) = 0, \quad (11)$$

$$u\left(\frac{L}{H}, y, t\right) = v\left(\frac{L}{H}, y, t\right) = 0, \quad (12)$$

$$u(x, 0, t) = v(x, 0, t) = 0, \quad (13)$$

$$u(x, 1, t) = v(x, 1, t) = 0, \quad (14)$$

$$\frac{\partial T}{\partial n}(0, y, t) = \frac{\partial T}{\partial x}(L, y, t) = 0, \quad (15)$$

$$\frac{\partial T}{\partial y}(x, 0, t) = \frac{\partial T}{\partial y}(x, H, t) = 0, \quad (16)$$

where L/H is the aspect ratio, and L is the length of the acoustic chamber. Figure 2 shows the rectangular chamber schematically.

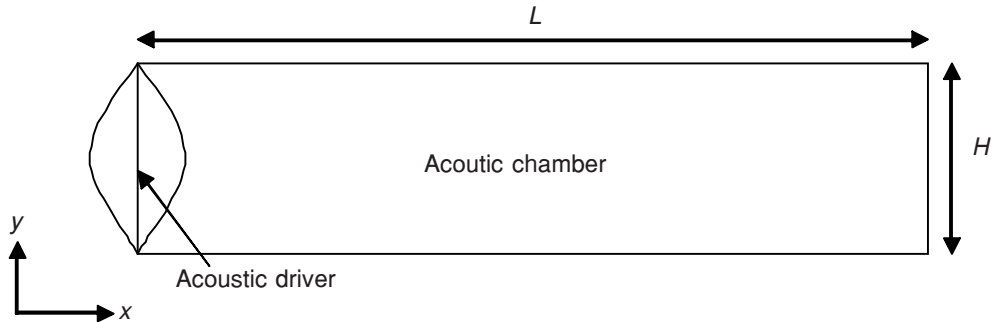


Figure 2 Schematic of the acoustic chamber

Waves are forced by imposing the normal component of velocity along one side of the vertical wall according to

$$u(0, y, t) = U_0 h(y) \sin t, \tag{17}$$

where U_0 is the forcing amplitude of the velocity and $h(y)$ is a shape function. Two shape functions have been employed; $h = 1$, which corresponds to a piston acoustic driver, and $h = \sin y$ which corresponds to a membrane, a typical acoustic driver used in practical thermoacoustic engines. Waves are forced into the chamber such that a half wavelength wave fits into the chamber length. Practical thermoacoustic chambers have either a quarter or half wavelength wave. This is because the temperature gradient desirable across the stack of heat exchanging plates within the chamber will not have fluctuations. This numerical method has been verified by comparing the computed results for the linear inviscid and viscous solutions to that of the analytical solutions [4].

4.0 RESULTS AND DISCUSSION

Computations are performed at Mach number of 40, Peclet number of 6×10^5 with a time-step of 0.001 for the length to height ratio of the acoustic chamber of 4 : 1. Simulations were completed over many cycles for both cases, membrane and piston acoustic driver. The temperature profiles at all Reynolds number attempted, 40, 100, 1000, and 8×10^5 , for both the membrane and piston agree with the linear inviscid theory. Figure 3 shows the inviscid theoretical half wavelength standing wave for both the velocity (thin) and temperature (thick) profiles at time t (gray) and half a cycle later (black).

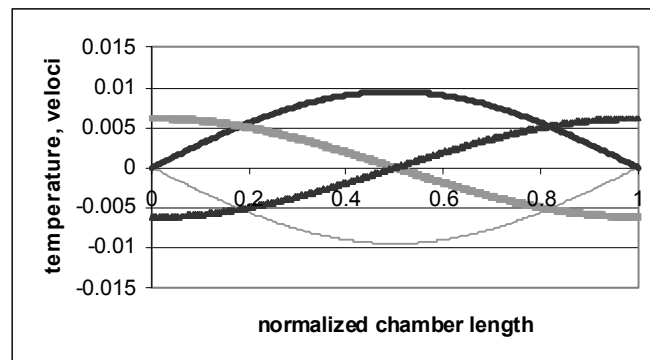


Figure 3 Theoretical standing wave temperature and velocity profiles

A half wavelength wave generated by the wave-maker in the simulation induced a temperature anti-node (maximum) close to the wall and temperature node (minimum) midway through the chamber, shown here in Figures 4 through 7. The profiles shown

here are computed at the chamber centerline so that there will be no boundary effects. Computational results are plotted at $t = 9.426$ (thin gray line), $t = 12.568$ (thick gray), $t = 25.136$ (thin black line), and $t = 28.278$ (thick black). The temperature nodes and anti-nodes obtained in this study agree well with past theoretical and experimental works [6,7] as can be seen when compared with figure 3. The stack and heat exchangers in practical thermoacoustic chamber are normally located near the wall, somewhere between a temperature node and anti-node.

Figure 4 shows an obvious increase in amplitude with time for both the membrane and piston driver. A high Reynolds number almost leading to an inviscid situation provides no resistance to the continuously generated acoustic waves into a lossless chamber resulting in increasing amplitude of the velocity and temperature. Theoretically the amplitude should increase as in this study but it is difficult to prove experimentally since it is near impossible to create a perfectly insulated acoustic chamber. As the Reynolds number is decreased, however, the temperature amplitude remains low and unchanged as seen here in Figure 7 where profiles at different times coincide. Energy is lost due to viscous effects and acoustic streaming within the moving fluid. The former is a widely accepted phenomena while the latter is a secondary flow associated with acoustic waves in a closed chamber [1,4,8].

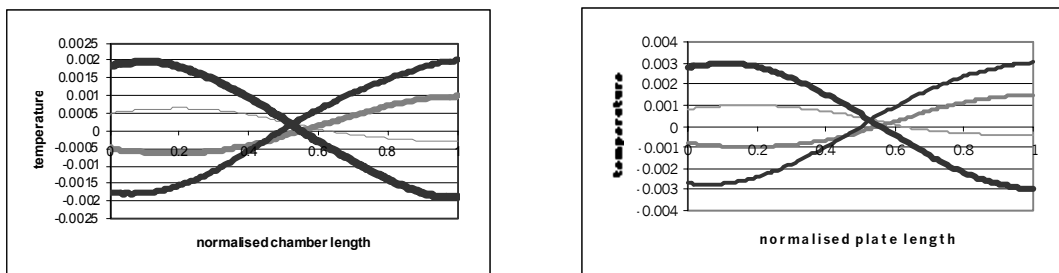


Figure 4 Temperature profiles at Reynolds number of 800 000 for membrane (left) and piston (right)

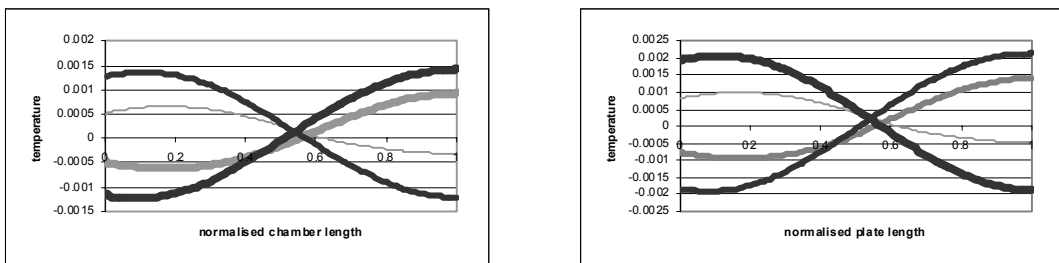


Figure 5 Temperature profiles at Reynolds number of 1000 for membrane (left) and piston (right)

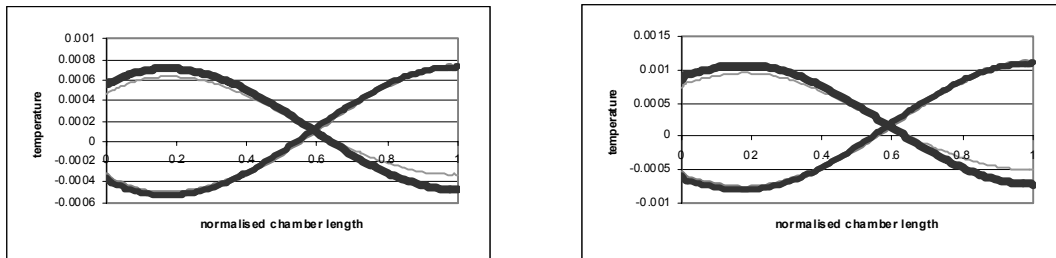


Figure 6 Temperature profiles at Reynolds number of 100 for membrane (left) and piston (right)

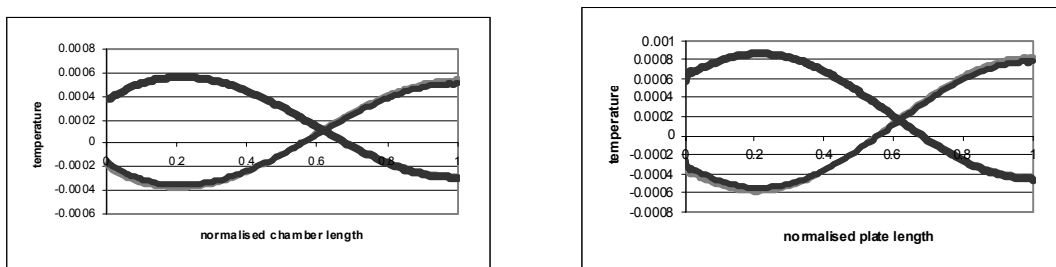


Figure 7 Temperature profiles at Reynolds number of 40 for membrane (left) and piston (right)

Although the forcing amplitude of the acoustic driver velocity for both the membrane and the piston is the same, the temperature amplitude computed at the same time frame is higher for the case of the piston. A piston does produce more boundary work than a membrane during an expansion/compression process due to its larger forces per unit area. The velocity amplitude generated by a piston is constant over the chamber height over time whilst that produced by a membrane is less except at the centerline.

5.0 CONCLUSION

Numerical simulation of acoustic waves in a rectangular chamber was completed with both the membrane and piston acoustic driver. The temperature profiles obtained agree with those of the linear inviscid theory. Viscosity is found to have a damping effect on the amplitude and a piston driver produced more work than the membrane. The next step in the study would be to study the relationship between the computed velocity and temperature profiles with increasing forcing amplitude of the acoustic driver. It has been reported that for higher perturbation to mean pressure ratio than 3%, nonlinearity effects begin to influence the behavior of acoustic waves in an enclosure.

REFERENCES

- [1] Strutt, J. W. 1945. *The Theory of Sound*, 2nd ed., Vol. II, New York: Dover.
- [2] Swift, G. W. 1988. Thermoacoustic Engines. *J. Acoust. Soc. Am.* 94(2): 1145-1179.
- [3] Bejan, A. 1995. *Convection Heat Transfer*. John Wiley.

- [4] Mohd-Ghazali, N. 2001. *Numerical Simulation of Acoustic Waves in a Rectangular Chamber*. Ph.D. thesis. University of New Hampshire at Durham, New Hampshire, USA.
- [5] Anderson, D. A., Tannehill, J. C., and Pletcher, R. H. 1984. *Computational Fluid Mechanics and Heat Transfer*. Taylor & Francis.
- [6] Beranek, L. L. 1954. *Acoustics*. New York: McGraw-Hill.
- [7] Swift, G. W. July 1995. Thermoacoustic Engines and Refrigerators. *Physics Today*.
- [8] Chini, G. 2001. Personal communications at Dept. Mech. Engineering, University of New Hampshire-Durham, New Hampshire.